**Title**
Aquifer Characterization by Passive Monitoring: A Case Study



**Author**
Hildenbrand, K.

**Publication Date**
1997-11-17

LBNL-41086
UC-400
Preprint

**ERNEST ORLANDO LAWRENCE BERKELEY NATIONAL LABORATORY**

# Aquifer Characterization by Passive Monitoring: A Case Study

Keary Hildenbrand and T.N. Narasimhan
**Earth Sciences Division**

November 1997
Submitted to
*Water Resources Research*

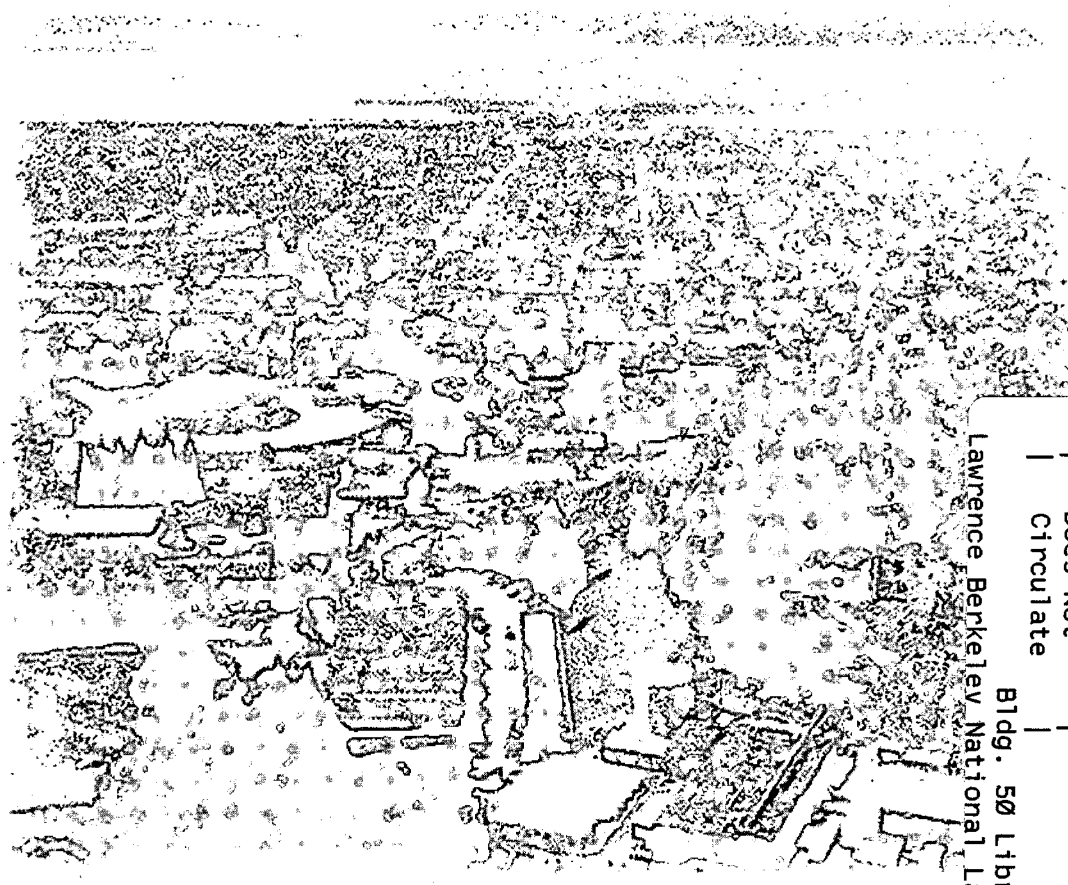

## DISCLAIMER

LBNL-41086
UC-400

# AQUIFER CHARACTERIZATION BY PASSIVE MONITORING: A CASE STUDY

KEARY HILDENBRAND
Presently at the Department of Earth and Environmental Science
New Mexico Institute of Mining and Technology
New Mexico, 87801

and

T.N. NARASIMHAN
Department of Materials Science and Mineral Engineering
Earth Sciences Division, Ernest Orlando Lawrence Berkeley National Laboratory
University of California at Berkeley
467 Evans Hall, Berkeley, 94720-1760

November, 1997

This work was partly supported by the Director, Office of Energy Research, Office of Basic Energy Sciences, U.S. Department of Energy under Contract No. DE-AC03-76SF00098.

# AQUIFER CHARACTERIZATION BY PASSIVE MONITORING: A CASE STUDY

KEARY HILDENBRAND[1] AND T. N. NARASIMHAN[2]

Department of Materials Science and Mineral Engineering
Earth Sciences Division, Ernest Orlando Lawrence Berkeley National Laboratory
University of California at Berkeley
467 Evans Hall, Berkeley, CA 94720-1760

## Abstract

With the availability of electronic data loggers, passive monitoring of water level changes in wells due to barometric variations and earth tides becomes an increasingly viable approach to hydraulically characterize aquifers. In a study to evaluate the utility of passive monitoring, water level data were collected over a one month period from wells penetrating confined aquifers at the Lawrence Livermore National Laboratory in California. Based on existing theoretical methods to analyze the response of aquifers to barometric changes and earth tides, compressibility and specific storage of the aquifers were estimated from these field data. The results show that the relatively shallow confined aquifers (at a depth of 40 to 50 meters below the land surface) are surprisingly stiff. Barometric responses indicated a compressibility of about 4E-11 $Pa^{-1}$ for the aquifer materials which is an order of magnitude smaller than the compressibility of water. Earth tide responses indicated a range of 2E-10 to 2E-9 $Pa^{-1}$, depending on the method used. This range is of the same order of magnitude as water compressibility. One would have expected a shallow, Quaternary material to be at least one to two orders of magnitude more compressible than water. It is not clear whether the material itself is stiff or whether the estimates reflect limitations of the analysis techniques. A pumping test conducted earlier on one of the aquifers yielded compressibility and specific storage estimates comparable with those estimated from earth tide response. Also, different techniques used to analyze the aquifer response to earth tides led to different estimates of compressibility and specific storage. Using the estimated values of compressibility and specific storage, the observed field data were dynamically simulated using a numerical model and credible matches were obtained between the simulations and the observations. In order to obtain the match, it was necessary to use different values of compressibility to generate pore pressure response due to barometric changes on the one hand and due to areal strains caused by earth tides on the other. The compressibility value associated with earth tide response was also used for specific storage. The dynamic simulations yielded well

---

[1] Presently at the Department of Earth and Environmental Science, New Mexico Institute of Mining and Technology, Socorro, New Mexico, 87801
[2] To whom correspondence must be addressed

constrained estimates for compressibility but yielded only a lower bound for hydraulic conductivity. The present study has shown that: (1) Passive monitoring can provide better estimates of the elastic properties of the aquifer than hydraulic conductivity whereas conventional pumping tests provide better estimates of hydraulic conductivity than elastic properties, (2) An aquifer may respond with different compressibilities to barometric changes on the one hand and depletion in storage due to pumping on the other, and, (3) Study of the passive response of more field systems may provide us with new insights about the elastic behavior of aquifers.

## Introduction

Water levels in wells screened in confined aquifers at the Lawrence Livermore National Laboratory (LLNL) consistently show effects of barometric changes and earth tides. Because these responses provide clues about the elastic properties of the aquifer material, measurements of barometric changes and water level fluctuations in five wells were recorded over a period of one month. The data were gathered between February and March, 1994. This study is an attempt to estimate the hydraulic characteristics of the aquifers penetrated by the wells by analyzing the passive monitoring data. The goal is partly to understand the efficacy of the different methods of analysis, partly to understand the properties of the specific aquifers and partly to understand the utility of passive monitoring data as a means to evaluate hydraulic characteristics of aquifers.

The approach we took in analyzing passive monitoring data is as follows. One-dimensional, vertical-strain assumption was used for the analysis of barometric effects. These effects were subtracted from the water level data, based on an estimate of the barometric efficiency. From the residuals, unexplained background trends were removed using two separate filtering processes. The remaining signals were treated as responses to earth tides. The interpretation of these earth tide effects required knowledge of areal strains (as suggested by Bredehoeft (1967)). In the absence of areal strain measurements at the site, a computer program by Harrison (1971) was used to estimate the theoretical areal strains occurring at the LLNL site based on a whole earth deformation model. Four different methods (suggested by previous researchers) were used to analyze the earth tide effects. Finally, as a synthesis, a numerical model was used to dynamically simulate the observed water level changes by combining barometric effects, earth tide effects, an unexplained trend, and transient groundwater flow. Additional details relating to this paper can be found in Hildenbrand (1995).

## Site Description

LLNL is located about 65 kms east of San Francisco, in the southeastern part of the Livermore Valley as shown in Figure 1. The valley is filled with 1200 m of Tertiary/Quarternary sediments of Pliocene to Holocene age, derived from the erosion of neighboring geologic formations. The deposits comprise a heterogeneous mixture of sand, gravel, silt, and clay. In a generally fine-grained host, irregular sand and gravel lenses deposited by meandering streams occur as interconnected permeable zones. The direction of flow of the streams is towards the west-northwest. Data from drilling logs (Qualheim, 1988) suggest that these sand lenses are elongated in the direction of stream flow and are generally a few hundred to a thousand meters long, tens to a few hundred meters wide, and a few meters thick (Schroth and Narasimhan, 1997). The aquifers discussed in the present study comprise part of these interconnected sand bodies.

The five wells monitored as part of the present study are located in the southwest corner of LLNL, off the right bank of Arroyo Seco (Table 1, Figure 2). The completion data for these wells and their average depth to water level (DTW) are given in Table 2. An idealized profile of the aquifers and the wells is shown in Figure 3. Wells MW-267, EW-712, and MW-616 pierce a 3-m thick lower aquifer while wells MW-214 and MW-264 pierce an upper aquifer of about the same thickness. The two aquifers are separated by another aquifer and aquitards. Although not shown in Figure 3, similarly thick clays and sands are known from the lithological logs to overlie the upper aquifer. In all the wells, the water level occurred 20 to 30 meters above the top of the aquifers. Based on this observation, we treat the aquifers as fully confined. By definition, a confined aquifer is such that, "In a well penetrating such an aquifer, the water level will rise above the bottom of the confining bed..." (Todd, 1980).

The 0.228 meter diameter boreholes were reportedly rotary drilled (air or mud). All wells were constructed with PVC pipe with a 0.114 meter inner diameter and slotted screens at the bottom. The outside of the casing was sealed with 5% bentonite and 95% cement above a sand pack directly outside the screen. The wells were screened in the most permeable aquifer in the formation and hence are treated as fully penetrating for purposes of this study.

Because the wells were constructed for purposes of environmental remediation, several different types of instruments have been installed within the wells. For instance, the wells are fitted with multistage submersible pumps, with the discharge pipe conveying the effluent to a nearby treatment facility. The diameter of the discharge pipe in the monitoring wells (e.g. MW 616) is 0.032 meters and 0.044 meters in the extraction well (EW-712). All wells were outfitted with stand pipes for collecting water level data. The outer and inner diameters of the stand pipes are 0.029 meters and 0.025 meters, respectively. Pressure transducers were set below the water level in the stand pipes to monitor water column fluctuations above the transducer. The wells are closed with the exception of the stand pipe which is open to the atmosphere. A sketch of the well instrumentation is given in Figure 4.

Natural water level fluctuations in five wells and barometric pressure changes were measured with pressure transducers from February 14, 1994, to March 18, 1994, and recorded with a data logger every 30 minutes. Between March 2, 1994, and March 4, 1994, equipment failure resulted in a gap in data. Hand measurements with an electric water level sounder were made periodically to check if the transducers were properly functioning. Nearby wells were not pumped during the monitoring period.

For comparison with natural water level fluctuation data, the barometric pressure data were converted to units of head, in meters of water. Note that a goal of the present study is to correlate *changes* in barometric pressure to *changes* in water level. Therefore, an average head value was first estimated and this average was removed from the data to obtain a measure of time-dependent changes. The data for each of these wells and barometer are given in Figures 5A through 5F. Figure 6 illustrates the inverse relationship between the barometric pressure changes and the changes in water levels in wells using EW-712 as an example. An increase in barometric pressure causes a drop in water level and vice versa.

## Interpretation Methodology

### *Response to Barometric Pressure*

We first analyze the relationship between barometric changes and water level fluctuations. Recall that barometric pressure and water levels in wells are inversely related as shown in Figure 6. Therefore for ease of comparing barometric pressure data with water level data, the barometric pressure data are first inverted; that is, the sign is reversed. Figure 7 shows the usefulness of inverting the barometric pressure data for correlation.

To evaluate the extent of correlation between existing water level changes and barometric pressure changes, the inverted barometric pressure data were multiplied by a number between 0 and 1 until the fluctuations reasonably match those of the water level data as demonstrated in Figure 8. This number is the barometric efficiency $B_E$. By definition, tidal efficiency $T_E = 1 - B_E$, where $B_E$ is barometric efficiency. The tidal efficiency is related to vertical aquifer compressibility [coefficient of volume change (Lambe and Whitman, 1969)] $m_v$ by,

$$m_v = \frac{T_E n\beta}{1 - T_E} \quad , \tag{1}$$

where n is porosity and $\beta$ is compressibility of water. Once $m_v$ is estimated the specific storage $S_s$ can be found using,

$$S_s = \rho g (m_v + n\beta) \quad , \tag{2}$$

in which, $\rho$ is density of water and g is acceleration due to gravity.

To facilitate earth tide analysis, barometric effects are removed by subtracting from the water level data the inverted barometric pressure data multiplied by the barometric efficiency. What is left are the earth tide effects and other signals.

***Response to Earth Tides***

In order to interpret water level response of the well to earth tides, it is first necessary to know the magnitude of earth strains caused by earth tides. In the absence of actual strain measurements in situ at LLNL, we may, as an expediency, use theoretically estimated strains in the manner suggested by Bredehoeft (1967). For this purpose, a computer program developed by Harrison (1971) is used in the present study. This tide program is based on average elastic properties of the whole earth. To relate the computed strains to pressure or water level changes, a constitutive equation needs to be derived. To this end, stress-strain relationships are described below to provide a foundation for determining hydraulic properties from the response of an aquifer to earth tides.

Consider a volume element fully saturated with water, subject to two-dimensional horizontal changes in external stress and three-dimensional deformation under "undrained" conditions (Bredehoeft, 1967). To facilitate analysis, we separately consider elastic deformations caused by external stress changes and by water pressure and superimpose the two effects. The net strains are the sum of the strains due to changes in external stress and water pressure. Noting that $\Delta\sigma_3 = 0$ if the Earth's surface is assumed to be a free surface, we get the following expression for net strains based on Hooke's Law,

$$\varepsilon_{1,net} = \frac{\Delta\sigma_1}{E} - \nu\frac{\Delta\sigma_2}{E} - \frac{(1-2\nu)}{E}\Delta p \ , \tag{3a}$$

$$\varepsilon_{2,net} = \frac{\Delta\sigma_2}{E} - \nu\frac{\Delta\sigma_1}{E} - \frac{(1-2\nu)}{E}\Delta p \ , \tag{3b}$$

and $$\varepsilon_{3,net} = -\frac{\nu}{E}(\Delta\sigma_1 + \Delta\sigma_2) - \frac{(1-2\nu)}{E}\Delta p \ , \tag{3c}$$

where, $\varepsilon_1$, $\varepsilon_2$ and $\varepsilon_3$ are linear strains, $\sigma_1$, $\sigma_2$ and $\sigma_3$ are principal stresses, E is Young's modulus and $\nu$ is Poisson's ratio. The net volumetric strain is the sum of the individual net strains, $\varepsilon_1 + \varepsilon_2 + \varepsilon_3$,

$$\varepsilon_{v,net} = \frac{(1-2\nu)}{E}(\Delta\sigma_1 + \Delta\sigma_2) - \frac{3(1-2\nu)}{E}\Delta p \ . \tag{4}$$

Under undrained response associated with earth tides, the net volumetric strain is equal to the change in water volume per unit bulk volume when the grains are assumed incompressible. Thus,

$$\frac{(1-2\nu)}{E}(\Delta\sigma_1 + \Delta\sigma_2) - \frac{3(1-2\nu)}{E}\Delta p = n\,\beta\,\Delta p \ . \tag{5}$$

If the lateral stresses are rewritten in terms of the areal strain ($\varepsilon_1 + \varepsilon_2$), Young's modulus rewritten in terms of the vertical compressibility, and the equation rearranged, we get,

$$m_v = \frac{(1-2\nu)}{(1-\nu)}\frac{\varepsilon_{a,net}}{\Delta p} - n\beta \ , \tag{6}$$

where $\varepsilon_{a,net} = \varepsilon_{1,net} + \varepsilon_{2,net}$. This is equivalent to the equation derived by Bredehoeft in 1967 and by Hsieh et al. in 1988. In using (6) for practical analysis, the areal strain $\varepsilon_{a,net}$ is obtained from the tide program based on a whole earth model, whereas the pressure changes are obtained by field measurements. Additionally, the compressibility of water is assumed to be 4.18E-10 $Pa^{-1}$. Under these circumstances, if one can assume reasonable values for n and ν, one may first estimate $m_v$ and then estimate $S_s$ based on (2).

### *Other Methods of Earth Tide Analysis*

It is instructive to compare the logic used in deriving (6) with the findings of other researchers (Roeloffs (1996), Rojstaczer and Agnew (1989), and Beavan et al. (1991)), who have looked at the response of aquifers to earth tides and barometric pressure changes.

Roeloffs' (1996) analysis is based on using volumetric strain, grain compressibility, and undrained Poisson's ratio $\nu_u$ defined through,

$$\Delta p = -\frac{2GB}{3\rho g}\frac{1+\nu_u}{1-2\nu_u}\varepsilon_{v,net} \ , \tag{7}$$

where the shear modulus G is related to the bulk modulus K by,

$$K = \frac{2G(1+\nu)}{3(1-2\nu)} \ . \tag{8}$$

Under conditions of compressible grains, Skempton's coefficient B is defined as (Rice and Cleary, 1976),

$$B = \frac{\frac{1}{K} - \frac{1}{K_s}}{\frac{1}{K} - \frac{1}{K_s} + n\left(\beta - \frac{1}{K_s}\right)} \quad , \tag{9}$$

where, $K_s$ is the bulk modulus (reciprocal of compressibility) of the solid grains. The negative sign in (7) arises because Roeloffs defines the barometric efficiency to vary between -1 and 0 instead of between 0 and 1. Two-dimensional loading and three-dimensional deformation are the basic principles behind the earth tide analysis given in (7). For analysis of aquifer response to barometric pressure changes the static confined barometric efficiency $E_B$ is given as,

$$E_B = -\left(1 - \left(\frac{B}{3}\right)\frac{1+\nu_u}{1-\nu_u}\right) \quad , \tag{10}$$

where it is assumed that areal strains are negligible for barometric pressure loading. Once $E_B$ is determined from barometric pressure and water level data then B can be calculated from (10) assuming a $\nu_u$. Then B can be substituted into (7) to determine G which can be converted to $m_v$. The results determined using Roeloffs' stress-strain equation will differ from those determined using Bredehoeft's approach because Roeloffs includes grain compressibility and uses undrained Poisson's ratio.

Rojstaczer and Agnew (1989) also include grain compressibility and undrained Poisson's ratio in their equations. Their equation based on two-dimensional loading and three-dimensional deformation is,

$$\Delta p = \frac{B}{\beta}\frac{1-2\nu_u}{1-\nu_u}\varepsilon_{a,net} \quad , \tag{11}$$

with B defined as in (9) and undrained compressibility is defined as,

$$\bar{\beta} = \alpha_{inv}(1-\alpha B) \ , \tag{12}$$

where, $\alpha_{inv}$ is 1/K and,

$$\alpha = 1 - \frac{K}{K_s} \ . \tag{13}$$

The static confined barometric efficiency is given as,

$$E_B = 1 - \frac{2B}{3}(1+\nu_u) \ , \tag{14}$$

assuming that the areal strains induced by barometric pressure loading are not negligible. After determining $E_B$ from barometric pressure and water level data, B can be estimated using (14) assuming a $\nu_u$. B can then be inserted into (11) to estimate $\bar{\beta}$. Using (12) and (13) K can then be determined to estimate $m_v$. Rojstaczer and Agnew (1989) also defined the one-dimensional specific storage coefficient as,

$$S_s = \rho g \left\{ \frac{\alpha}{K}\left[1 - \left(\frac{2\alpha(1-2\nu)}{3(1-\nu)}\right)\right] + n\left(\beta - \frac{1}{K_s}\right) \right\} \ , \tag{15}$$

which takes into account grain compressibility. The results derived from Rojstaczer and Agnew will be similar to those of Roeloffs' method because they both include undrained Poisson's ratio and grain compressibility. The slight difference will be due to the $E_B$ equation, because Rojstaczer and Agnew include the areal strains due to barometric pressure loading.

Beavan et al. (1991) used areal strains and a parameter $d\varepsilon_{a,net}/dP_B$ to describe barometric pressure loading. The parameter is usually assumed to equal zero but Beavan et al. considered models with values other than zero. For the "layer over half-space" model, $d\varepsilon_{a,net}/dP_B$ = 7.6E-12

$Pa^{-1}$, and for the spherical layered model, $d\varepsilon_{a,net}/dP_B$ = 4.2E-12 $Pa^{-1}$. Their earth tide analysis equation based on two-dimensional loading and three-dimensional deformation is,

$$G = \frac{A_t}{\frac{2}{\rho g}(1 - B_E) - 2A_t \frac{d\varepsilon_{a,net}}{dP_B}} , \tag{16}$$

where tidal admittance $A_t$ is defined as,

$$A_t = \frac{\Delta p}{\rho g \varepsilon_{a,net}} . \tag{17}$$

The loading efficiency $\gamma$ is given as,

$$\gamma = (1 - B_E) - \rho g A_t \frac{d\varepsilon_{a,net}}{dP_B} . \tag{18}$$

and equals the tidal efficiency $T_E$ if $d\varepsilon_{a,net}/dP_B = 0$. The specific storage, $S_s^*$ is defined as,

$$S_s^* = \frac{\rho g}{\gamma(1-\nu)}\left[\frac{1-2\nu}{2G} - \frac{1+\nu}{3K_s}\right] , \tag{19}$$

which also includes grain compressibility. Beavan et al. (1991) determined that the results did not significantly differ when including the lateral strains due to barometric loading. Beavan et al. use exactly the same stress-strain relation as Roeloffs when assuming $d\varepsilon_{a,net}/dP_B = 0$. Their specific storage equation differs from (15) because of assuming $d\varepsilon_{a,net}/dP_B = 0$, and differs from (2) because it includes grain compressibility.

Overall, the aquifer hydraulic properties estimated using Bredehoeft's equation will probably be an upper limit because Bredehoeft neglects grain compressibility, undrained Poisson's ratio, and areal strains from barometric pressure loading. The hydraulic properties estimated by applying all of the above methods to data from a single should be within a small range because all of the methods are based on using theoretical areal strains as well as the same boundary conditions.

### *Filtering Techniques*

After removal of the barometric effects from the water level data as described earlier, a zero phase shift, high-pass filter by Pertsev (1957) was applied to water level data from which barometric effects had been removed. For data sampled every half hour, the filtered data were calculated using,

$$\Delta\overline{p}(t) = \Delta p(t) - \frac{1}{15}\sum_{n=1}^{15}\Delta p(t+i_n) \quad , \tag{20}$$

where $i_n$ = (-36, -26, -20, -16, -10, -6, -4, 0, 4, 6, 10, 16, 20, 26, 36) in half hours. This equation is based on a simple moving average filter and removes any long periods. It was assumed that the "high-pass" output was the water level changes due to earth tides. An example of the application of the high-pass filter to water level data from well EW-712 is given in Figure 9.

The other filter is a least-squares filter (Quilty and Roeloffs, 1996). It was used to calculate the best-fitting barometric efficiency using linear regression. After removing barometric effects, a least-squares method was used to determine the amplitudes and phases of sine and cosine waves with periods of the tidal constituents that best fit the data (Table 3). Therefore, the earth tide water level changes are approximated by the sum,

$$\frac{\Delta p_{et}}{\rho g} = \sum_{n=1}^{N}\left(a_n\cos(\omega_n t_n) + b_n\sin(\omega_n t_n)\right) \quad , \tag{21}$$

where $t_n$ is the time of the nth data point, $\omega_n$ is the frequency of the nth tidal constituent, and $a_n$ and $b_n$ are unknown coefficients. The sum is taken over the total number of tidal constituents, N.

The unknowns, $a_n$ and $b_n$, are calculated using the method of least squares to best fit the water level data. Accordingly, the amplitude and phase of the nth tidal constituent are,

$$\text{amp}_n = \sqrt{(a_n)^2 + (b_n)^2} \quad , \tag{22}$$

$$\text{phase}_n = \tan^{-1}\left(\frac{b_n}{a_n}\right) \quad . \tag{23}$$

The sum of these waves with periods of the tidal constituents, calculated amplitudes, and calculated phases is the total water level change due to earth tides. An example of the separation of the three effects is given in Figure 10 for well EW-712.

The next step is to correlate water level changes due to earth tides obtained from either filter with the areal strains estimated theoretically from a whole earth model. The earth tide water level changes arising due to earth tides from the least-squares filter is given as an example in Figure 11 for well EW-712. In order to compute aquifer compressibility and specific storage, the values at the peaks and troughs of the strains and water levels that were in phase were read off and inserted into the earth tide equations and the parameters were backed out.

The theoretical areal strains were also processed by the least-squares filter to determine the amplitudes and phases of the individual tidal constituents. These amplitudes were used with those determined with the water level data to estimate aquifer hydraulic properties. Only the $M_2$ and $O_1$ tides were chosen for interpretation because they are entirely due to the lunar cycle and are not contaminated by barometric effects.

### *Numerical Simulation*

To complement the estimation of aquifer hydraulic properties already outlined, a full simulation of the aquifer response to barometric pressure and earth tides was accomplished using the numerical model TRUST (Narasimhan et al., 1978). TRUST is a computer program which helps analyze transient flow of water in a variably-saturated, deformable, multi-dimensional heterogeneous porous media under isothermal conditions, based on the Integral Finite Difference (IFD) scheme. The user designs the geometric assemblage of the volume elements so as to best approximate the expected flow pattern for improved accuracy. The associated integral expressions which are solved using matrix methods, represent conservation of mass over each of the three-dimensional volume elements. The IFD uses first order approximation for determining spatial gradients of potential.

For the present study, TRUST was modified to handle two types of source terms. The first, conventional source term, pertains to addition or removal of water, as is the case, for example, of a well. The second pertains to pore pressure generation associated with undrained loading, as in the case with barometric effects or earth tide response of an aquifer. For purposes of this study, ocean tides were neglected since LLNL is quite removed from the ocean. In the simulations, permeability, fluid viscosity, porosity and compressibility of geologic material and compressibility of water were provided as input. Hydraulic conductivity and specific storage are not explicitly specified. Tidal efficiency, needed to convert barometric pressure changes into pore pressure generation, was calculated from the input values of compressibility.

## Results

### *Response to Barometric Pressure Changes*

The barometric pressure data were inverted and multiplied by a number between 0 and 1 ($B_E$) to visually best fit with the water level data for each well. Data from wells EW-712, MW-616, MW-267, and MW-214 yielded the best fit for $B_E = 0.70$ and $T_E = 0.30$. In view of (1) and (2) and assuming $n = 0.25$ and $\beta = 4.18E\text{-}10\ Pa^{-1}$, $B_E = 0.70$ yields $m_v = 4.48E\text{-}11\ Pa^{-1}$ and $S_s = 1.46E\text{-}6\ m^{-1}$. Data from well MW-264 yielded the best fit for $B_E = 0.75$ and $T_E = 0.25$ which resulted in $m_v = 3.48E\text{-}11\ Pa^{-1}$ and $S_s = 1.37E\text{-}6\ m^{-1}$. Note that these estimates of aquifer compressibility ($\approx 4E\text{-}11\ Pa^{-1}$) are an order of magnitude smaller than the compressibility of water. One would normally expect alluvial materials to be far more compressible than water, say, in the range, $10^{-9}$ to $10^{-7}\ Pa^{-1}$; but data from these wells are consistent with a compressibility an order of magnitude smaller than that of water.

### *Response to Earth Tide Effects*

The responses of the aquifers to strains induced by earth tides were analyzed in two different ways. The first was a gross analysis of the combined effects of all 8 tidal components based on a visual comparison of the similarities between the peaks and troughs of water level variations and areal strain variations with time. The second was an analysis of the responses of the aquifers to two specific tidal components by comparing the water level amplitude corresponding to the areal strain amplitude due to a particular tidal component.

First let us consider the gross analysis. The water level changes due to earth tides isolated by each filter were plotted with the theoretical areal strains (calculated using average Love numbers of H = 0.6007 and L = 0.0766). For both filters, the peaks and troughs of the water levels reasonably match those of the areal strains. The largest amplitudes of the peaks and troughs of the earth tide effects were used to estimate the aquifer hydraulic properties by inserting these amplitudes into (6) and (2) (assuming $n = 0.25$, $\nu = 0.25$, and $\beta = 4.18E\text{-}10\ Pa^{-1}$). Average compressibility was calculated from about twelve such peaks and troughs. The average compressibility and specific storage for each filter using the method of Bredehoeft for each well is given in Table 4. The overall average compressibility and specific storage are, approximately, 2E-10 $Pa^{-1}$ and 3E-6 $m^{-1}$, respectively. These values are about five times larger than those determined from the barometric pressure analysis ($m_v$ = 4E-11 $Pa^{-1}$, $S_s$ = 1E-6 $m^{-1}$), but the estimated compressibility is still about half that of water.

A few sensitivity experiments were conducted to evaluate the effects of porosity and Poisson's ratio on the estimated compressibility values. An areal strain of 1E-08 and a pressure change of 13 Pa were used. At a Poisson's ratio of 0.25, the estimated compressibility varied linearly from 4.8E-10 $Pa^{-1}$ at $n = 0.1$ to 3.6E-10 $Pa^{-1}$ at $n = 0.4$. At a porosity of 0.25, the compressibility was found to vary linearly from 4.8E-10 $Pa^{-1}$ at $\nu = 0.2$ to 1.6E-10 $Pa^{-1}$ at $\nu = 0.4$. Thus, the estimated compressibilities are not very sensitive to porosity or Poisson's ratio.

Now let us consider the response of the aquifers to individual tidal components. The amplitudes and phases of the $M_2$ and $O_1$ constituents of the water levels and the theoretical areal strains were first determined using the least-squares filter. In order to evaluate how closely these two were related to each other, their $M_2/O_1$ amplitude ratios are compared Table 5. The $M_2/O_1$ amplitude ratio for the water levels and that for tide-induced strains differ notably between each other. Here, it should be noted that the strain amplitude and phase information pertaining to water levels are being compared with theoretical strains from the whole earth model. They should properly be compared with actual measurements at the site, which, unfortunately, are not available. As pointed out by Berger and Beaumont (1976), theoretical strains can differ from actual strains by as much as 50%. In a confined aquifer, one would expect the water levels and strains to have the same phase, provided that the permeability of the aquifer is reasonably large. Also, one would expect that the water levels in wells in the same aquifer would have the same phase and amplitude ratio. The differences in phases and amplitude ratios between theoretical strains and measured water levels probably reflect the uncertainties involved in matching filtered field data against theoretically computed strains. The differences could also be due to the fact that the earth tide effects are small compared to the barometric effects and that uncertainty reflects the errors inherent in extracting small periodic signals from a large composite signal.

The amplitudes of water levels and areal strains corresponding to $M_2$ and $O_1$ tidal components were analyzed using the methods of Bredehoeft (1967), Rojstaczer and Agnew (1989), Beavan et al. (1991) and Roeloffs (1996). The results, obtained assuming $K_s$ = 4.95E10 Pa, n = 0.25, $\nu = \nu_u = 0.25$, and $\beta$ = 4.18E-10 $Pa^{-1}$, are summarized in Table 6. As can be seen, compressibility estimates using Bredehoeft's approach yielded the largest values among all the methods used. Also, comparison with results presented in Table 4 indicates that the estimates based on a visual comparison of the peaks and troughs of the water levels and areal strains are significantly smaller by a factor of 3 to 5.

The compressibility values estimated with the method of Beavan et al. were the same as those obtained with the method of Roeloffs (1996) because it was assumed that loading due to barometric pressure in the lateral directions was negligible. Although Rojstaczer and Agnew (1989) accounted for lateral strains in response to barometric changes, their estimates of compressibility are not significantly different from those of Roeloffs (1996) or Beavan et al. (1991). It is seen from Table 6 that the estimates based on Bredehoeft's method are in general about 3 times larger than those obtained using other methods.

In summary, we see that the analysis of earth tide response by the methods of Rojstaczer and Agnew (1989), Beavan et al. (1991) and Roeloffs (1996) yield compressibility values ranging from about 1E-10 to about 5E-10 $Pa^{-1}$. This range is compatible with the estimates obtained with the gross analysis using Bredehoeft's method. Application of the Bredehoeft method to $M_2$ and $O_1$ signals indicate a range of about 6E-10 to about 2E-9 $Pa^{-1}$ for aquifer compressibility, which is 1.5 to 5 times the compressibility of water. Based on these, it is reasonable to state that the aquifer materials are about as compressible as water as indicated by their response to earth tides.

### *Numerical Simulation*

For simulating the passive monitoring data, a radially symmetric mesh was used to model the aquifer system. The volume elements used are a sequence of concentric cylindrical shells around the well. Outward from the well are a sequence of volume elements with radii increasing by a factor of 1.25 out to about 1175 meters. A permeable zone was assumed out to 0.125 meters, to represent the sand pack surrounding the well casing. Provision was also made for a "skin" outside the gravel pack, to give consideration to aquifer damage during well completion. The unexplained trend determined from either filter was entered as input into TRUST for each well. The gap in the unexplained trend and barometric pressure data were filled in by a visual estimate of the regional trend so that the data are continuous. The barometric pressure data were also entered as input into TRUST.

To simulate the effects of barometric pressure and earth tides, time-dependent changes measured barometric pressure and theoretically computed areal strains were entered as tabulated inputs. Within the computational algorithm, barometric pressure changes and areal strains have to be converted to equivalent pore pressure changes according to (1) and (6) respectively. For this purpose, one has to specify, *a priori*, the compressibility of the aquifer material, $m_v$. However, as we have seen, analysis of barometric data yielded compressibility values an order of magnitude smaller than that indicated by earth tide analysis. Therefore, two separate compressibility values were entered as input, one for simulating barometric effects and the other for simulating earth tide effects and specific storage.

The fact that we had to use different values of compressibility for barometric effects and earth tide effects indirectly may suggest barometric efficiency and tidal efficiency does not add up to 1. One possible explanation for this might be that one has to give consideration to grain compressibility in the estimation. In our calculations we had assumed grains to be completely rigid. We know that grain compressibility will be unimportant only when the porous matrix is far more compressible than the solid grains. If indeed we have to account for grain compressibility in our case, the indirect implication is that the porous matrix is quite stiff.

In the simulations, six parameters were iteratively manipulated to match the computational output with the observed water level data. These are, aquifer compressibility (specific storage), aquifer permeability, sand pack permeability, sand pack specific storage, skin permeability, and skin specific storage. The compressibility value used for specific storage was also used to convert areal strains to pore pressure changes. An appropriate compressibility was used to effectively result in a tidal efficiency of 0.3 (i.e. barometric efficiency = 0.7) to convert barometric changes to pore pressure changes. This was done because barometric efficiency was very well constrained by the field data analysis.

The outputs of numerical simulations were insensitive to permeability and specific storage of the sand pack and skin. These permeability and specific storage values were varied over several orders of magnitude with no change in the output. Thus the aquifer compressibility and permeability were the principal parameters of calibration. A lower limit of the aquifer permeability, about $10^{-13}$ $m^2$, was determined since the output was insensitive with permeability values larger than this lower limit. Ultimately, therefore, only the compressibility (specific storage) of the aquifer proved responsive to calibration within a reasonable range. The range in specific storage for wells MW-264 and MW-214 was 3E-6 $m^{-1}$ to 6E-5 $m^{-1}$ with 6E-5 $m^{-1}$ being a reasonable value. This corresponds to a compressibility range of 2E-10 to 6E-9 $Pa^{-1}$ with 6E-9 $Pa^{-1}$ being a reasonable value . For wells MW-267, MW-616, and EW-712 $S_s$ 5E-6 $m^{-1}$ to 6E-5 $m^{-1}$ with 9E-6 $m^{-1}$ being a reasonable value. This corresponds to a range in compressibility of 4E-10 to 6E-9 $Pa^{-1}$ with 8E-10 $Pa^{-1}$ being a reasonable value. As an example, the matching results for well EW-712 is shown in Figure 11. Water levels from wells MW-264 and MW-214 could not be perfectly matched with the computed output of TRUST. This inability to converge on a reasonable result could be due to not accounting for some unknown signal or effect in the upper aquifer. However, data from wells EW-712, MW-616, and MW-267 which penetrate the lower aquifer were better amenable to matching with computational simulations.

In an earlier work, Schroth and Narasimhan (1997) used a numerical model to analyze data from a pumping test conducted on well EW-712. In their analysis, they simulated a two-aquifer system separated by an aquitard, with the lower being the pumped aquifer. In the calibration process they treated the aquitard to be more compressible than the aquifer. Under these assumptions, their analysis suggested a range of 1E-5 to 2E-5 $m^{-1}$ for specific storage for the lower aquifer, corresponding to a range of 9E-10 to 2E-9 $Pa^{-1}$ for compressibility. For the lower aquifer, the permeability ranged from 3E-12 to 5E-12 $m^2$ with 4E-12 $m^2$ being a reasonable value. A summary of estimated hydraulic properties by all of the methods is given in Table 7.

## Discussion

Application of the concept of undrained loading to an open well penetrating a confined aquifer leads to the inference that barometric efficiency should be close to zero if the aquifer material is relatively soft and compressible and that it should be close to 1 if the aquifer material is stiff and incompressible. Analysis of field data from the LLNL aquifers show that all five wells have indicated a barometric efficiency of about 0.7, without much uncertainty. Assuming a porosity of 0.25 and a water compressibility of 4.18E-10 $Pa^{-1}$, we find that this barometric efficiency corresponds to an aquifer compressibility that is an order of magnitude smaller than that of water.

It is interesting that all the methods used for interpreting the earth tide response of the aquifers have yielded fairly well-constrained estimates for compressibility and specific storage. The methods of Rojstaczer and Agnew (1989), Beavan et al. (1991) and Roeloffs (1996) yielded remarkably consistent compressibility estimates between 1E-10 and 5E-10 $Pa^{-1}$. A visual comparison of the filtered water level data with theoretically calculated areal strains followed by the application of the Bredehoeft method also yielded estimates of compressibility in the range, 1E-10 to 4E-10 $Pa^{-1}$. Somewhat higher estimates for compressibility (4E-10 to 2E-9 $Pa^{-1}$) were obtained when the Bredehoeft method was applied to two specific tidal components. Ignoring the extreme estimates, it is reasonable to state that the earth tide response of the aquifers have indicated that the aquifer materials have a compressibility varying from 1 to perhaps 3 times the compressibility of water. This estimate is also comparable to an estimate arrived at by Schroth and Narasimhan (1997) based on a pumping test.

These analysis show that the aquifer responds as a very stiff material to barometric stresses while it responds as a more soft material to earth tides and to pumpage of water. This apparent difference in behavior is intriguing. Secondly, even in the case of earth tides and groundwater pumping, the estimates of compressibility suggest that the aquifer material is not more than about thrice as compressible as water. It is not clear why a Quaternary alluvial material should appear so stiff. Does this imply a limitation in the method of analysis or is the aquifer material truly stiff due to special circumstances such as precipitation of cement at grain contacts?

Concerning the method of analysis itself, one could argue that the aquifer is actually unconfined and that the apparent stiffness is due to the fact that the aquifer has been treated as confined in the analysis. However the hydrogeologic conditions at the site are consistent with the aquifer being confined. Lithologic logs show that the sediments pierced by the wells contain many alternating layers of fine-grained and coarse-grained materials, with the fine-grained sediments acting as aquitards. And, in each of the wells water level rises to between 20 and 30 meters above the top of aquifers.

Another alternative worth considering is whether the apparent stiffness may be due to leakage of water from the aquitards. Aquitards are generally fine-grained sediments which are more compressible than aquifers and thus possess higher tidal efficiency. Thus, for a given increase in barometric pressure, more pore pressure will be generated in the aquitard than in the aquifer. Consequently, one should expect additional water to leak into the aquifer from the aquitard as barometric pressure increases and this leakage will be more rapid if the aquitard has relatively high hydraulic conductivity. If we follow this reasoning, it becomes clear that addition of excess water by leakage from the aquitard will increase the apparent tidal efficiency of the aquifer material and make it appear softer than what it really is. Therefore, it does not seem reasonable to suspect that the aquifers under consideration appear stiff because of leakage from the aquitard.

## Concluding Remarks

Passive monitoring of water levels in wells piercing confined aquifers have yielded remarkably well-constrained estimates of the compressibility of the aquifers under dynamic conditions using different sets of assumptions. More frequent use of passive monitoring methods to characterize groundwater systems may prove to be of great value, particularly because pumping tests yield reliable estimates of aquifer hydraulic conductivity but cannot be relied upon to give accurate estimates of specific storage. Thus, passive monitoring and pumping tests are complimentary tools of analysis for hydraulic characterization of groundwater systems.

The different compressibility estimates from barometric analysis and earth tide analysis suggests that aquifers may respond differently to different dynamic processes. The estimated hight stiffness of a shallow Quaternary aquifer at the Livermore site suggests that we have much to learn about the elastic behavior of aquifers. Passive monitoring methods are relatively inexpensive and are potentially capable of giving us new insights into aquifer dynamics.

## Acknowledgments

We would like to thank John Ziagos, Robert Gelinas and Eric Nichols (formerly of Weiss Associates) for the facilities afforded in gathering the data on which this work is based. We had the benefit of insightful discussions on earth tide processes with Evelyn Roeloffs, Stuart Rojstaczer, Paul Hsieh and John Bredehoeft. Computer programs and advice provided by John Harrison (earth tides), Tom Hildenbrand and Robert Jachens (time-series analysis) were invaluable in the furtherance of this work. Garth van der Kamp, Andrew Fisher, Ernest Majer, Evelyn Roeloffs and John Duey reviewed the manuscript and provided valuable criticisms.

Keary Hildenbrand gratefully acknowledges financial support from a Jane Lewis fellowship at the University of California at Berkeley. This work was partly supported by the Director, Office of Energy Research, Office of Basic Energy Sciences, U.S. Department of Energy under Contract No. DE-AC03-76SF00098.

# References

Beavan, B., K. Evans, S. Mousa, and D. Simpson, Estimating Aquifer Parameters From Analysis of Forced Fluctuations in Well Level: An Example From the Nubian Formation Near Aswan, Egypt, 2. Poroelastic Properties, *Journal of Geophysical Research, 96*, B7, 12139-12160, 1991.

Berger, J., and C. Beaumont, An Analysis of Tidal Strain Observations From the United States of America, II. The Inhomogeneous Tide, *Bulletin of the Seismological Society of America, 66*, 6, 1821-1846, 1976.

Bredehoeft, J. D., Response of Well-Aquifer Systems to Earth Tides, *Journal of Geophysical Research, 72*, 12, 3075-3087, 1967.

Freeze, R. A., and J. A. Cherry, *Groundwater*, 604 pp., Prentice Hall, Inc., Englewood Cliffs, New Jersey, 1979.

Harrison, J. C., New Computer Programs for the Calculation of Earth Tides, Report from the Cooperative Institute for Research in Environmental Sciences, University of Colorado, Boulder, 1971.

Hildenbrand, K.L., Hydraulic characterization of an aquifer through passive monitoring: A case study, M.S. dissertation, Department of Materials Science and Mineral Engineering, University of California at Berkeley, 149 p., 1995.

Hsieh, P. A., J. D. Bredehoeft, and S. A. Rojstaczer, Response of Well Aquifer Systems to Earth Tides: Problem Revisited, *Water Resources Research, 24*, 3, 468-472, 1988.

Narasimhan, T. N., A Unified Numerical Model for Saturated-Unsaturated Groundwater Flow, Ph.D. Dissertation, Department of Civil Engineering, University of California, Berkeley, 1975.

Pertsev, B. P., On the Calculation of the Drift Curve in Observations on Bodily Tides, *Bulletin d'informations, No. 5, Commission pour l'étude des Marées Térrèstres*, 71-72, 1957.

Qualheim, B. J., Well Log Report for the LLNL Ground Water Project: 1984-1987, *Environmental Protection/Environmental Restoration Series UCID-21342*, 1988.

Quilty, E. G., and E. A. Roeloffs, User's Guide to FORTRAN Programs for Analysis of Water Level Time Series Data, U. S. Geological Survey, 1995.

Rice, J.R. and M.P. Cleary, Some Basic Stress Diffusion Solutions for Fluid –Saturated Elastic Porous Media with Compressible Constituents, *Reviews of Geophys.*, 14, 227-241, 1976.

Roeloffs, E. A., Poroelastic Techniques in the Study of Earthquake-Related Hydrologic Phenomena, in *Advances in Geophysics*, Editor R. Dmowska, 37, 135-195, 1996.

Rojstaczer, S., and D. C. Agnew, The Influence of Formation Material Properties on the Response of Water Levels in Wells to Earth Tides and Atmospheric Loading, *Journal of Geophysical Research, 94*, B9, 12403-12411, 1989.

Seifert, P., Personal Communication, Lawrence Berkeley Laboratory, 1995.

Schroth, B., and T. N. Narasimhan, Technical Note: Application of a Numerical Model in the Interpretation of a Leaky Aquifer Test, *Ground Water*, 35(2), 371-375, 1997

Thorpe, R. K., W. F. Isherwood, M. D. Dresen, and C. P. Webster-Scholten (eds.), *CERCLA Remediation Investigation Report for the LLNL Livermore Site*, Environmental Restoration Division, Lawrence Livermore National Laboratory, Livermore, California, 1990.

Todd, D.K., Groundwater Hydrology, John Wiley and Sons, Second Edition, 1980.

Table 1: Location of wells.

| Well | North Latitude m | East Longitude m |
|---|---|---|
| MW-214 | 2963.03 | 1947.55 |
| MW-264 | 2853.43 | 2084.06 |
| MW-267 | 2878.73 | 1942.06 |
| MW-616 | 2964.55 | 1964.34 |
| EW-712 | 2918.62 | 1967.05 |

Table 2: Well completion and average depth to water table (DTW) data.

| Well | Ground Elevation m | Screen Top m | Screen Length m | DTW m | Elevation of Water Level m | Water Column Above Screen Top m |
|---|---|---|---|---|---|---|
| MW-214 | 182.28 | 141.45 | 2.29 | 21.58 | 160.70 | 19.25 |
| MW-264 | 183.62 | 140.66 | 3.05 | 23.38 | 160.24 | 19.58 |
| MW-267 | 182.38 | 129.81 | 1.98 | 21.70 | 160.68 | 30.87 |
| MW-616 | 182.51 | 128.25 | 3.05 | 22.59 | 159.92 | 31.67 |
| EW-712 | 182.48 | 130.66 | 4.72 | 22.60 | 159.88 | 29.22 |

Note: Elevations are with respect to mean sea level.

Table 3: The important tidal constituents and their periods.

| Tidal Constituent | Period, hours |
|---|---|
| $O_1$ | 25.8193 |
| $S_1$ | 24.0000 |
| $K_1$ | 23.9345 |
| $J_1$ | 23.0985 |
| $N_2$ | 12.6583 |
| $M_2$ | 12.4206 |
| $S_2$ | 12.0000 |
| $K_2$ | 11.9672 |

Table 4: Averages of peaks and troughs using Bredehoeft's (1967) equation.

| | Filter Type | $m_v$, $Pa^{-1}$ | $S_s$, $m^{-1}$ |
|---|---|---|---|
| MW-214 | Least-Squares | 1.34E-10 | 2.34E-06 |
| | High-Pass | 2.29E-10 | 3.27E-06 |
| MW-264 | Least-Squares | 2.51E-10 | 3.49E-06 |
| | High-Pass | 2.51E-10 | 3.49E-06 |
| MW-267 | Least-Squares | 2.38E-10 | 3.36E-06 |
| | High-Pass | 1.77E-10 | 2.76E-06 |
| MW-616 | Least-Squares | 2.71E-10 | 3.68E-06 |
| | High-Pass | 2.21E-10 | 3.19E-06 |
| EW-712 | Least-Squares | 3.30E-10 | 4.26E-06 |
| | High-Pass | 3.04E-10 | 4.01E-06 |

Table 5: Amplitudes and phases of water level changes and average strains.

| | | Amplitude (nanostrain) | Phase (°) | $M_2/O_1$ |
|---|---|---|---|---|
| Areal Strain | $M_2$ | 18.18 | 326 | 1.75 |
| h=.601, l=.077 | $O_1$ | 10.41 | 226 | |
| Volumetric Strain | $M_2$ | 12.12 | 326 | 1.75 |
| h=.601, l=.077 | $O_1$ | 6.94 | 226 | |

| | | Amplitude (mm) | Phase (°) | $M_2/O_1$ |
|---|---|---|---|---|
| MW-214 | $M_2$ | 0.843 | 117 | 0.60 |
| | $O_1$ | 1.416 | 48 | |
| MW-264 | $M_2$ | 0.871 | 144 | 2.40 |
| | $O_1$ | 0.363 | 167 | |
| MW-267 | $M_2$ | 1.645 | 125 | 3.27 |
| | $O_1$ | 0.503 | 147 | |
| MW-616 | $M_2$ | 1.589 | 126 | 3.55 |
| | $O_1$ | 0.448 | 157 | |
| EW-712 | $M_2$ | 1.600 | 129 | 3.38 |
| | $O_1$ | 0.474 | 137 | |

Note: $\varepsilon_{vol} = \frac{1-2\nu}{1-\nu}\varepsilon_a$ with $\nu = 0.25$.

Table 6: Aquifer hydraulic properties estimated using average strains and the method developed by the specified author(s); $M_2$ and $O_1$ amplitudes determined from the tidal analysis program.

| | Bredehoeft | | Rojstaczer & Agnew | | Roeloffs | | Beavan et al. | |
|---|---|---|---|---|---|---|---|---|
| $M_2$ | $m_v$ | $S_s$ | $m_v$ | $S_s^*$ | $m_v$ | $S_s$ | $m_v$ | $S_s^*$ |
| MW-214 | 1.36E-09 | 1.44E-05 | 4.36E-10 | 4.25E-06 | 4.30E-10 | — | 4.30E-10 | 1.40E-05 |
| MW-264 | 1.31E-09 | 1.39E-05 | 3.31E-10 | 3.22E-06 | 3.53E-10 | — | 3.53E-10 | 1.35E-05 |
| MW-267 | 6.47E-10 | 7.37E-06 | 2.11E-10 | 2.04E-06 | 2.14E-10 | — | 2.14E-10 | 6.98E-06 |
| MW-616 | 6.78E-10 | 7.67E-06 | 2.33E-10 | 2.26E-06 | 2.32E-10 | — | 2.32E-10 | 7.30E-06 |
| EW-712 | 6.68E-10 | 7.58E-06 | 2.27E-10 | 2.20E-06 | 2.26E-10 | — | 2.26E-10 | 7.20E-06 |

| $O_1$ | $m_v$ | $S_s$ | $m_v$ | $S_s^*$ | $m_v$ | $S_s$ | $m_v$ | $S_s^*$ |
|---|---|---|---|---|---|---|---|---|
| MW-214 | 3.95E-10 | 4.90E-06 | 1.44E-10 | 1.39E-06 | 1.46E-10 | — | 1.46E-10 | 4.53E-06 |
| MW-264 | 1.85E-09 | 1.91E-05 | 4.57E-10 | 4.45E-06 | 4.85E-10 | — | 4.85E-10 | 1.87E-05 |
| MW-267 | 1.30E-09 | 1.38E-05 | 4.00E-10 | 3.90E-06 | 4.01E-10 | — | 4.01E-10 | 1.34E-05 |
| MW-616 | 1.48E-09 | 1.55E-05 | 4.77E-10 | 4.66E-06 | 4.68E-10 | — | 4.68E-10 | 1.51E-05 |
| EW-712 | 1.39E-09 | 1.46E-05 | 4.44E-10 | 4.33E-06 | 4.37E-10 | — | 4.37E-10 | 1.43E-05 |

Table 7: Summary of the estimates of aquifer hydraulic properties.

| | $m_v$, $Pa^{-1}$ | $S_s$, $m^{-1}$ | k, $m^2$ |
|---|---|---|---|
| Atmospheric Pressure | 3.5E-11 - 4.5E-11 | 1.4E-06 - 1.5E-06 | |
| Earth Tides-match peaks | | | |
| High-Pass | 1.8E-10 - 3.0E-10 | 2.8E-06 - 4.0E-06 | |
| Least-Squares | 1.3E-10 - 3.3E-10 | 2.3E-06 - 4.3E-06 | |
| Earth Tides-Bredehoeft | | | |
| $M_2$ | 6.8E-10 - 1.4E-09 | 7.7E-06 - 1.4E-05 | |
| $O_1$ | 4.0E-10 - 1.9E-09 | 4.9E-06 - 1.4E-05 | |
| Earth Tides-Beavan et al. | | | |
| $M_2$ | 2.1E-10 - 4.3E-10 | 7.0E-06 - 1.4E-05 | |
| $O_1$ | 1.5E-10 - 4.9E-10 | 4.5E-06 - 1.9E-05 | |
| Earth Tides-Roeloffs | | | |
| $M_2$ | 2.1E-10 - 4.3E-10 | | |
| $O_1$ | 1.5E-10 - 4.9E-10 | | |
| Earth Tides-Rojstaczer & Agnew | | | |
| $M_2$ | 2.1E-10 - 4.4E-10 | 4.3E-06 - 2.0E-06 | |
| $O_1$ | 1.4E-10 - 4.8E-10 | 1.4E-06 - 4.7E-06 | |
| TRUST- Passive Test | 2.0E-10 - 6.0E-09 | 3.0E-06 - 6.0E-05 | 1.0E-13 - 1.0E-08 |
| TRUST-Pumping Test | 9.2E-10 - 1.9E-09 | 1.0E-05 - 2.0E-05 | 3.0E-12 - 5.0E-12 |

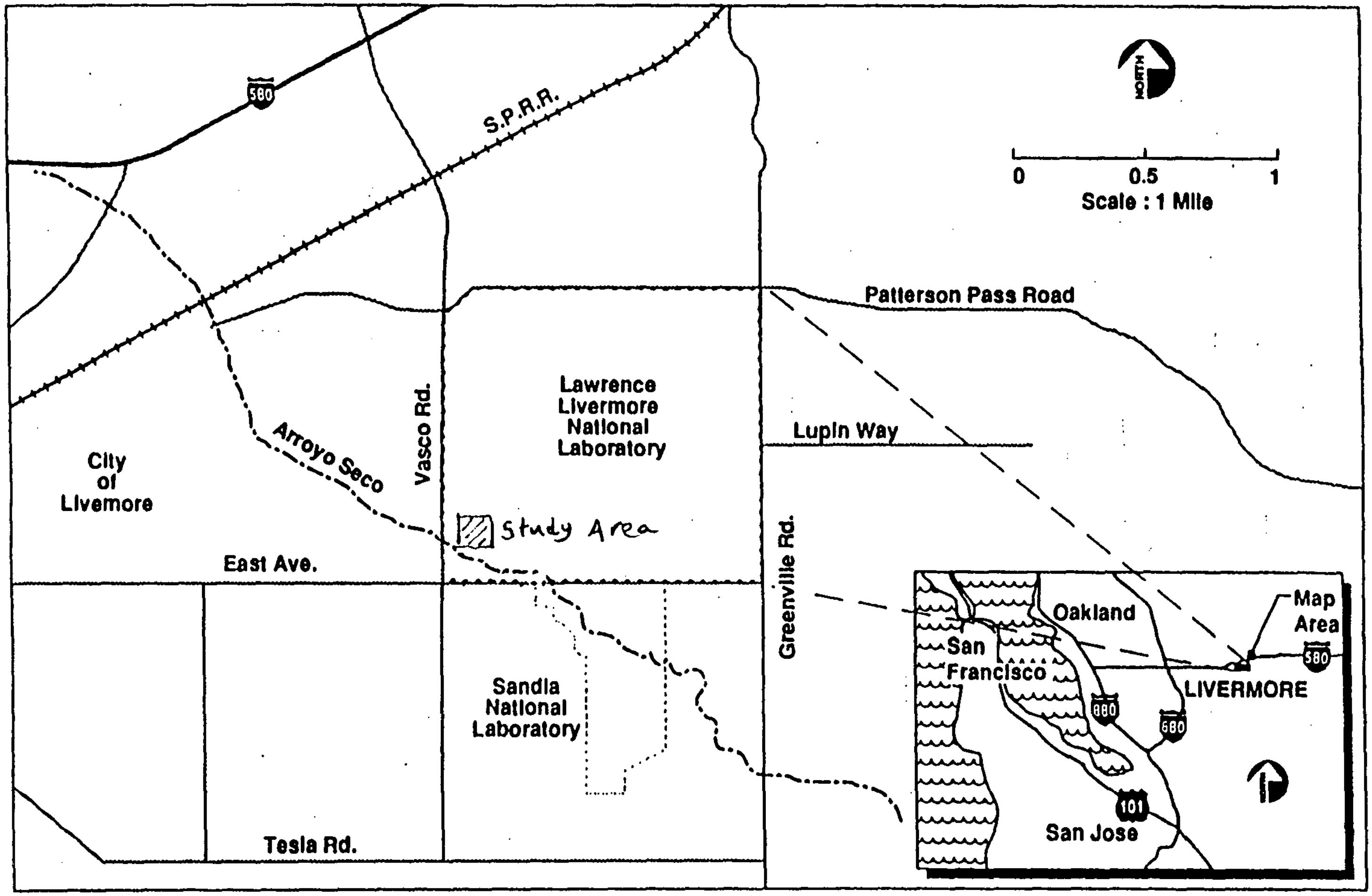


Figure 1: Location map of the Lawrence Livermore National Laboratory.

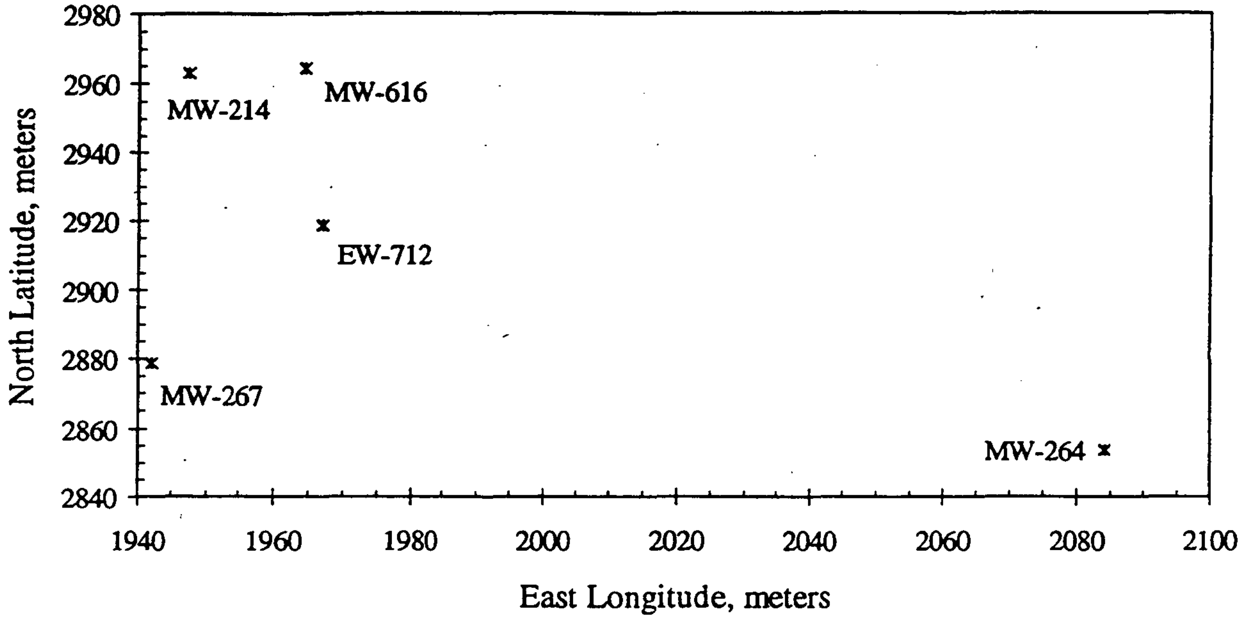


Figure 2: Location of the wells monitored for the present study.

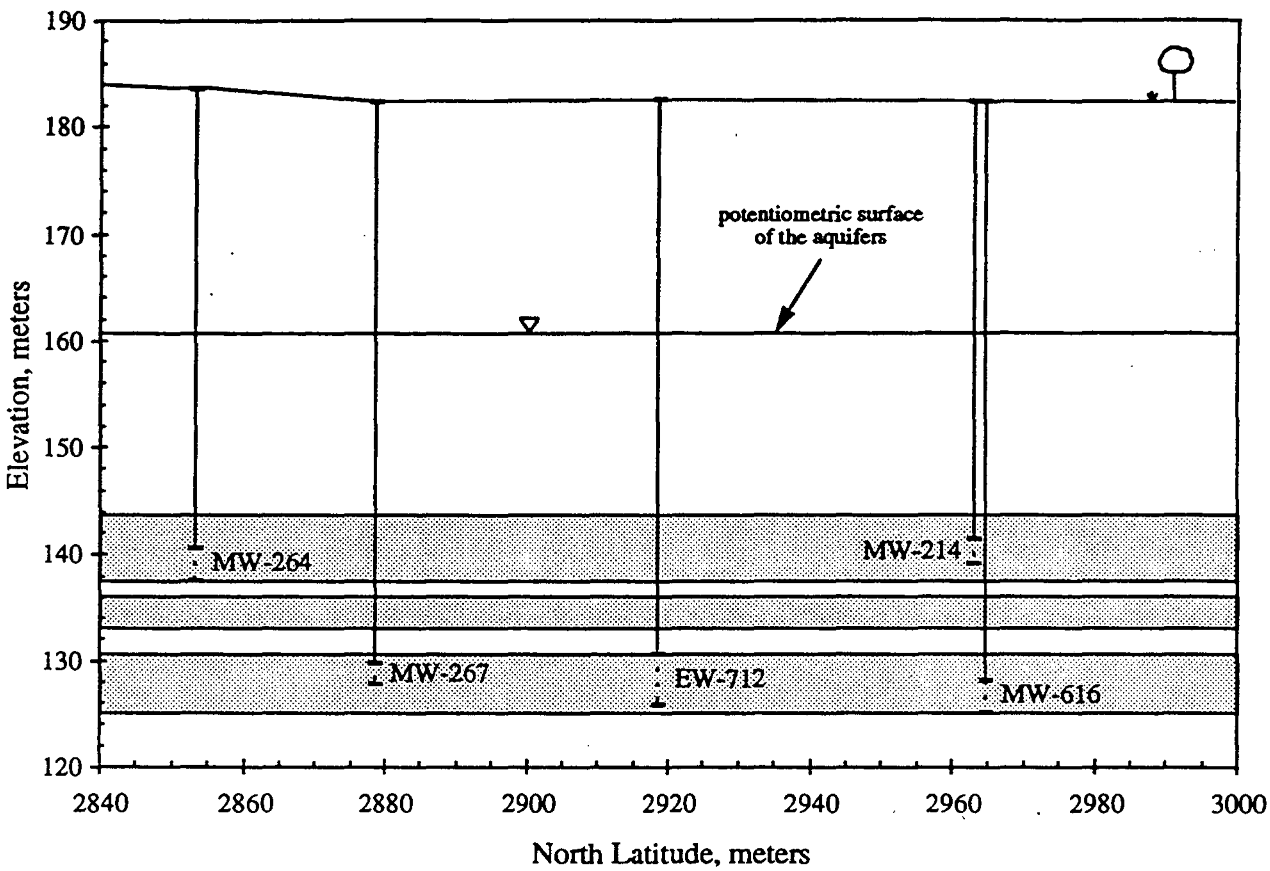


Figure 3: Idealized profile of the leaky-aquifer system.

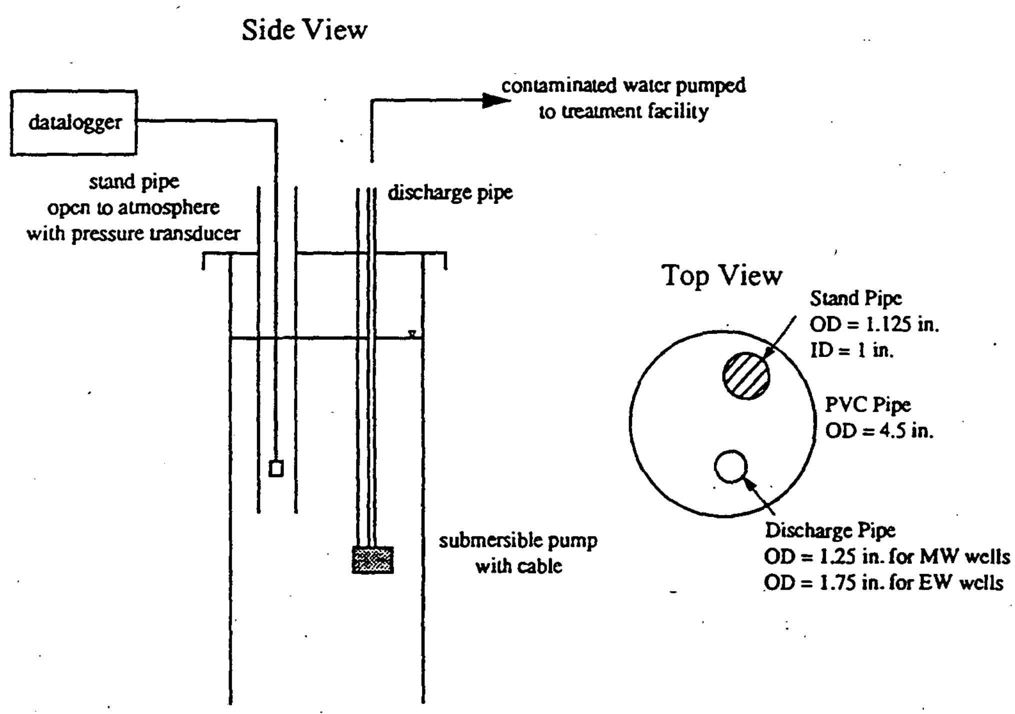


Figure 4: Sketch of well instrumentation.

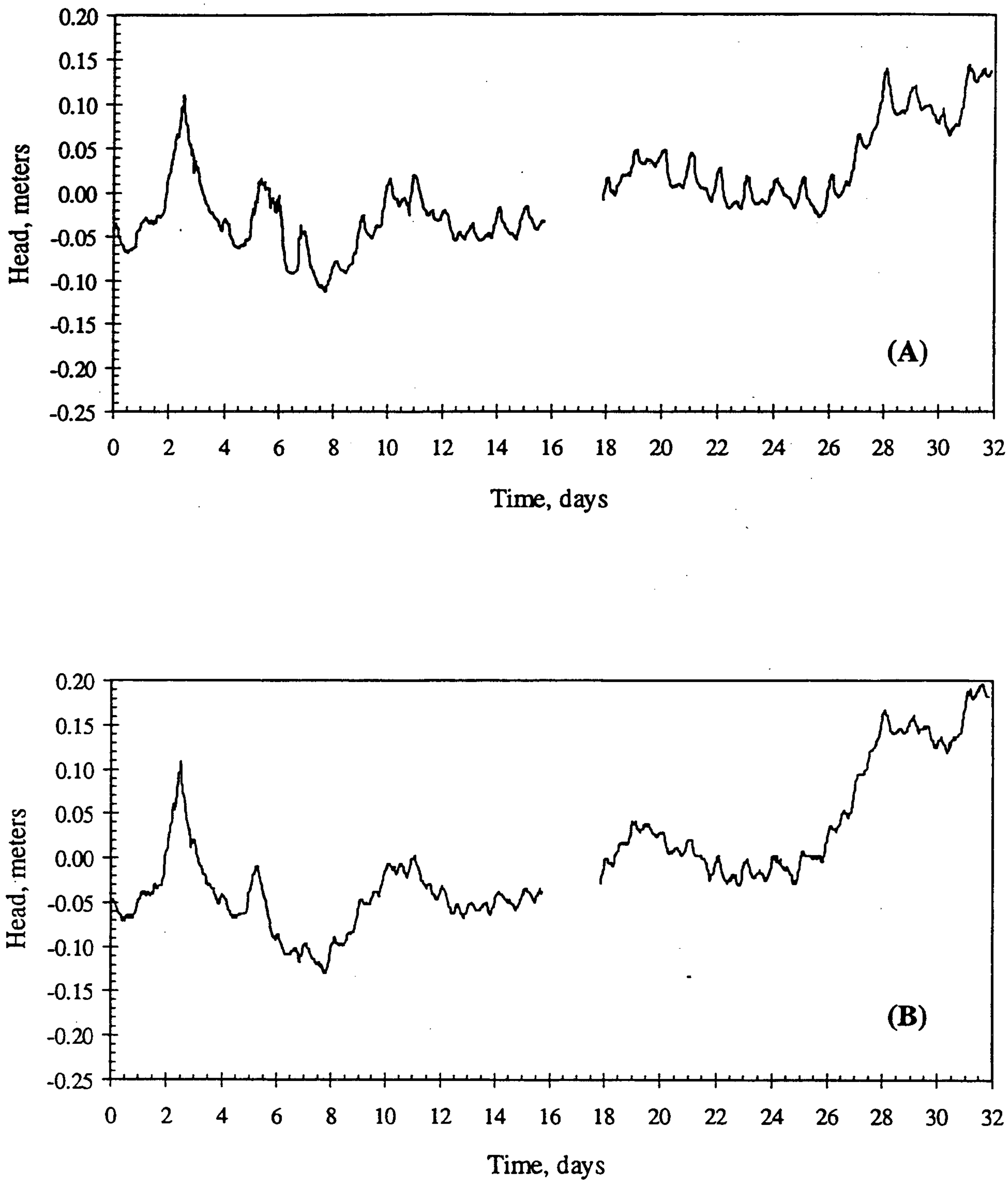


Figure 5: Natural water level fluctuations for wells; (A) MW-214 and (B) MW-264.

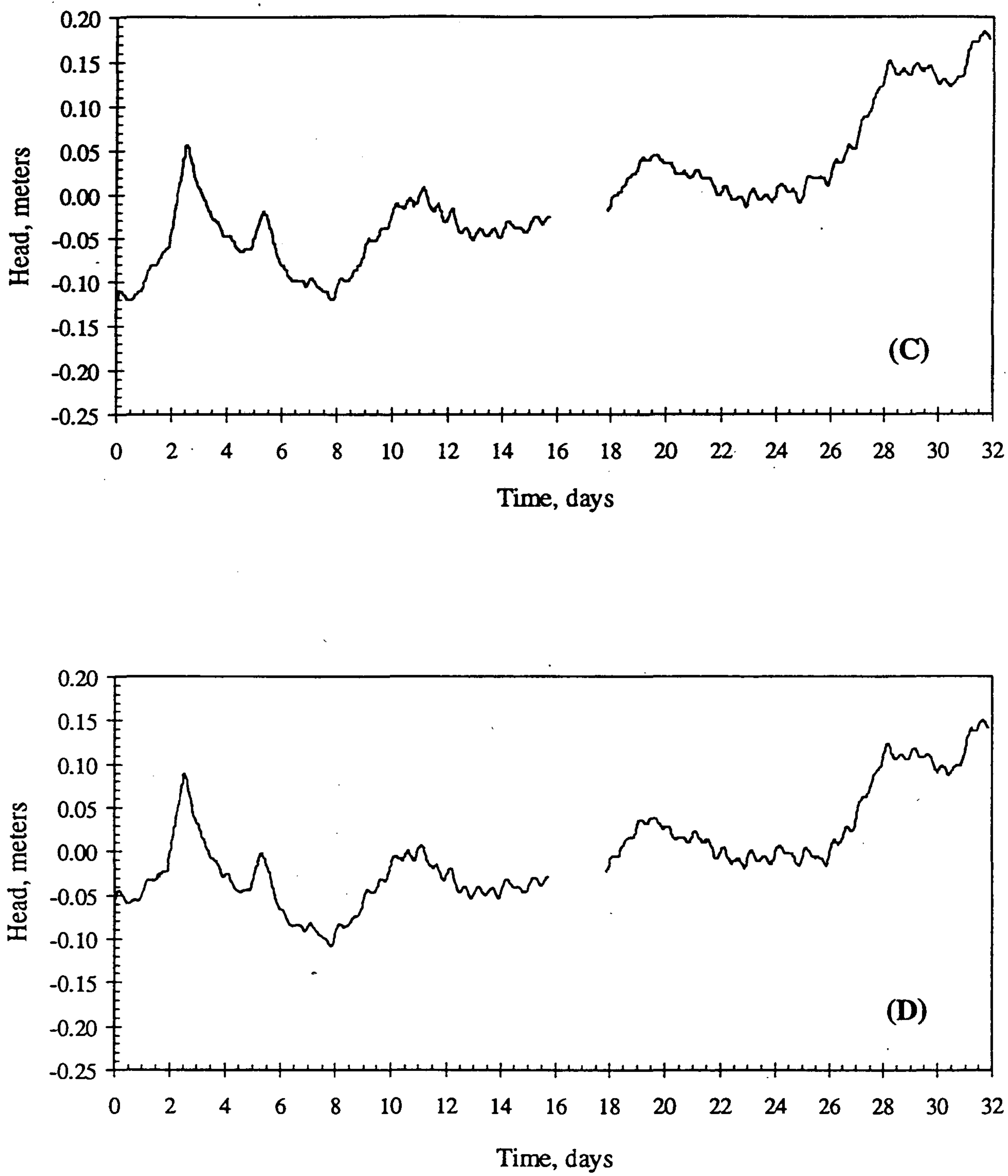


Figure 5: Natural water level fluctuations for wells; (C) MW-267 and (D) MW-616.

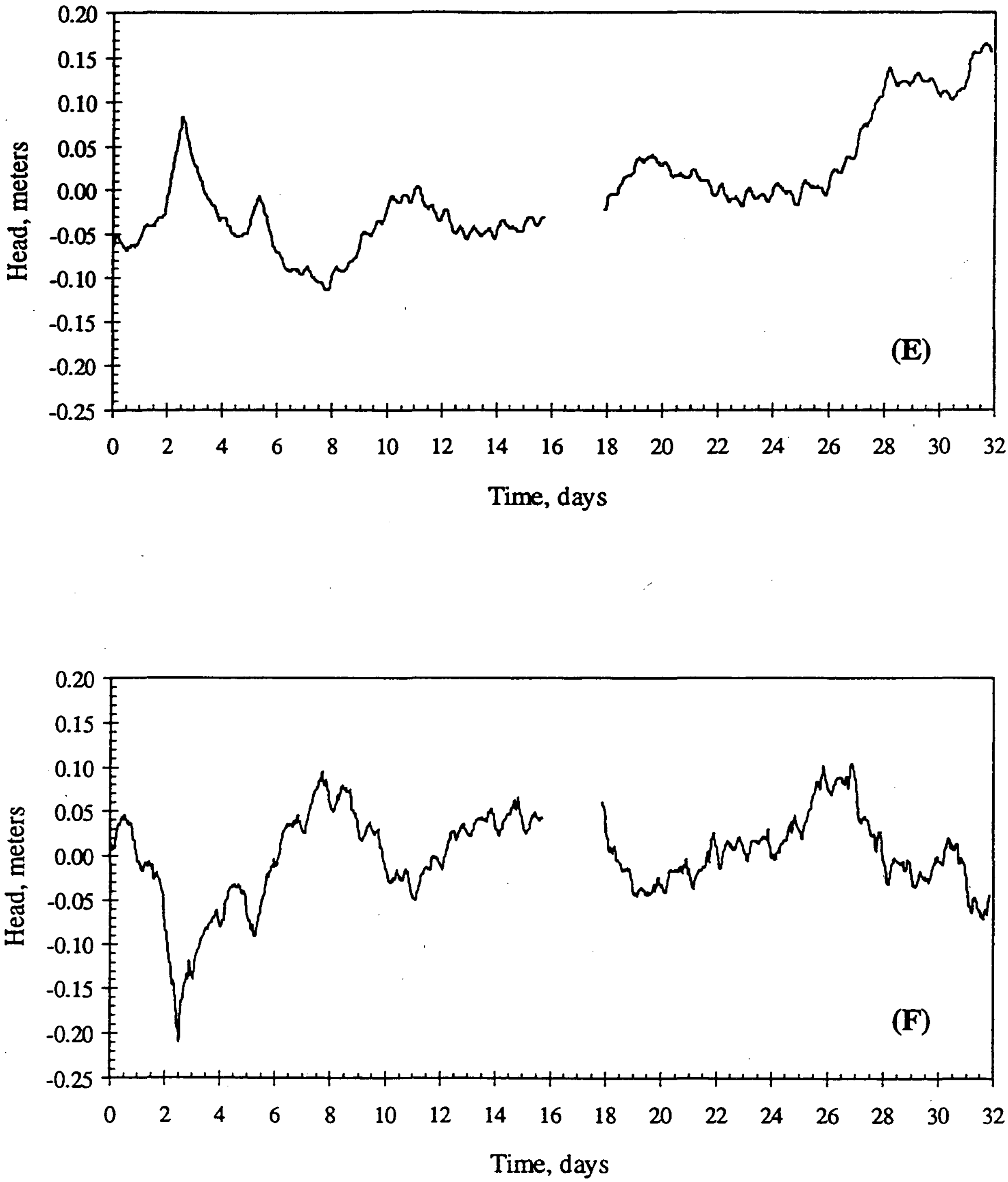


Figure 5: Natural water level fluctuations for (E) well EW-712 and (F) barometer.

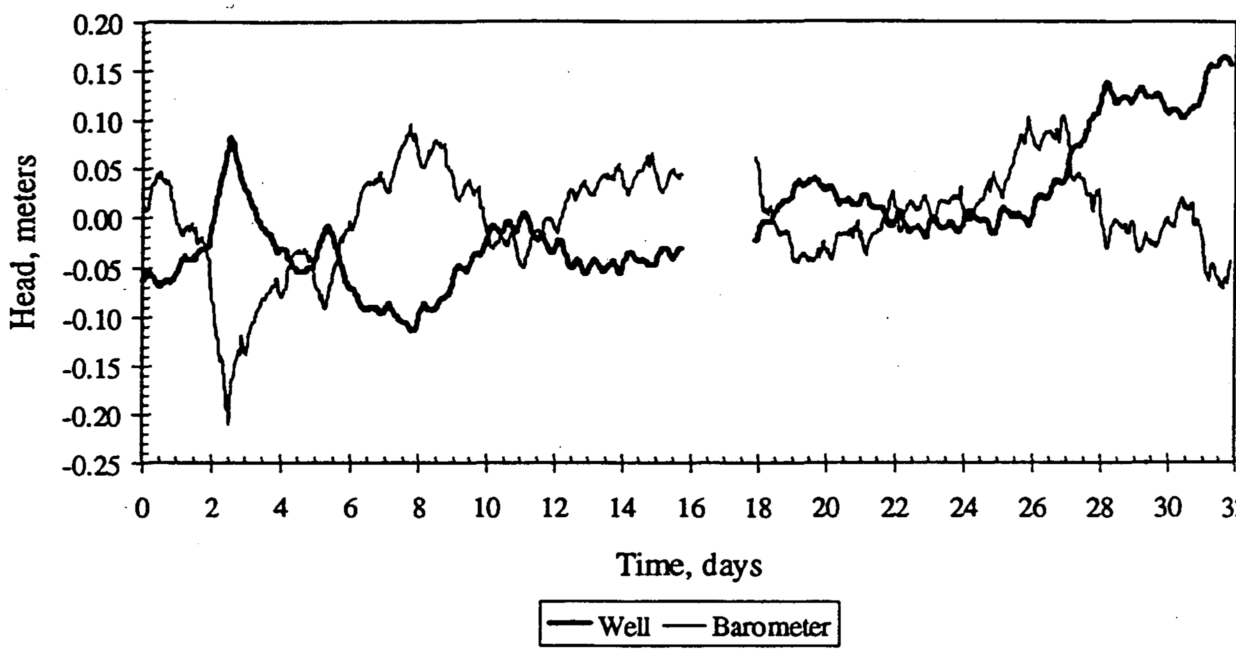


Figure 6: Inverse relation between barometric changes and water levels for well EW-712.

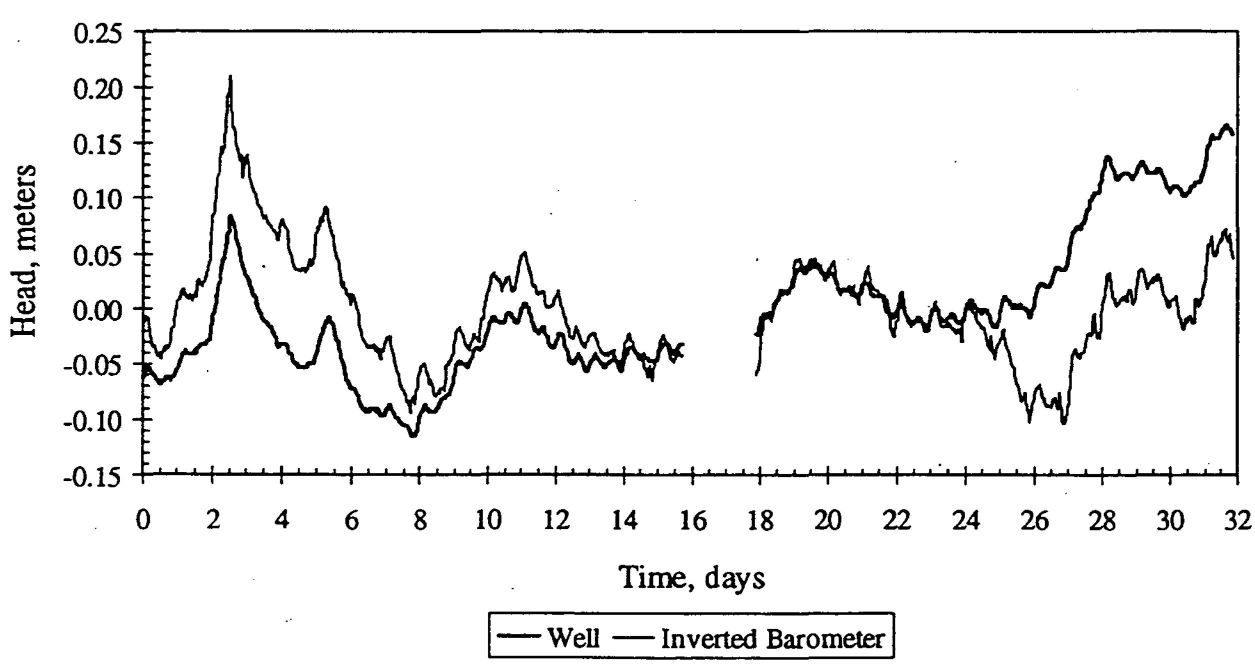


Figure 7: Inverted barometric changes and water levels in well EW-712.

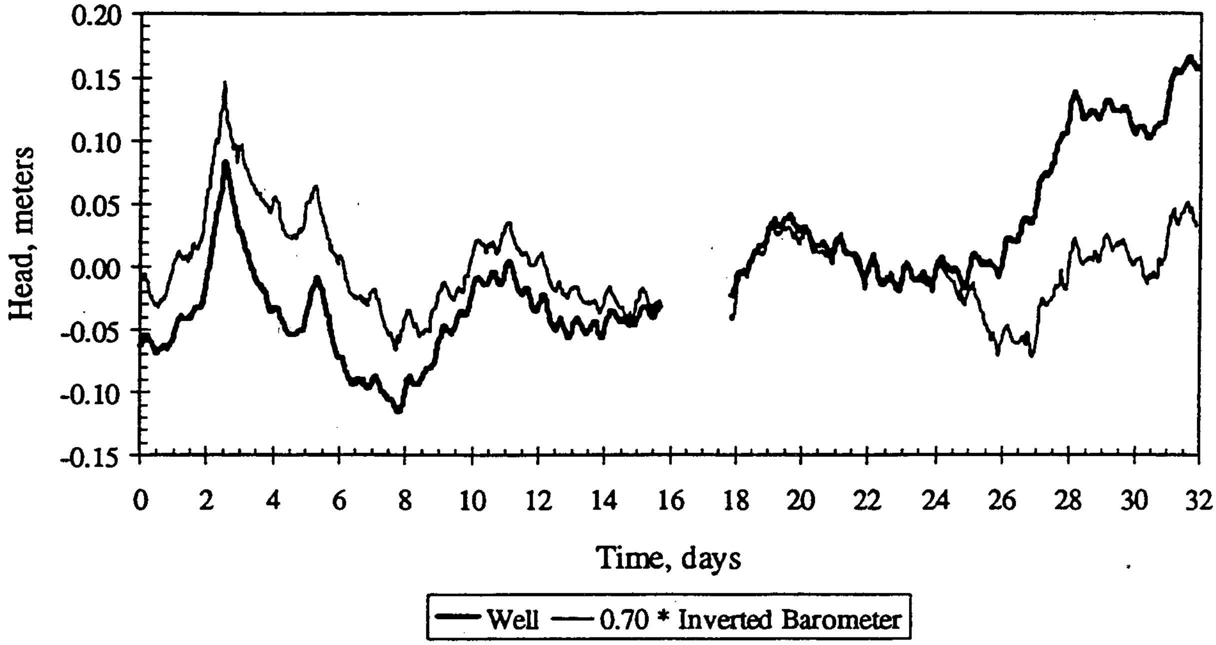


Figure 8: Barometric efficiency times the inverted barometer and water levels in well EW-712.

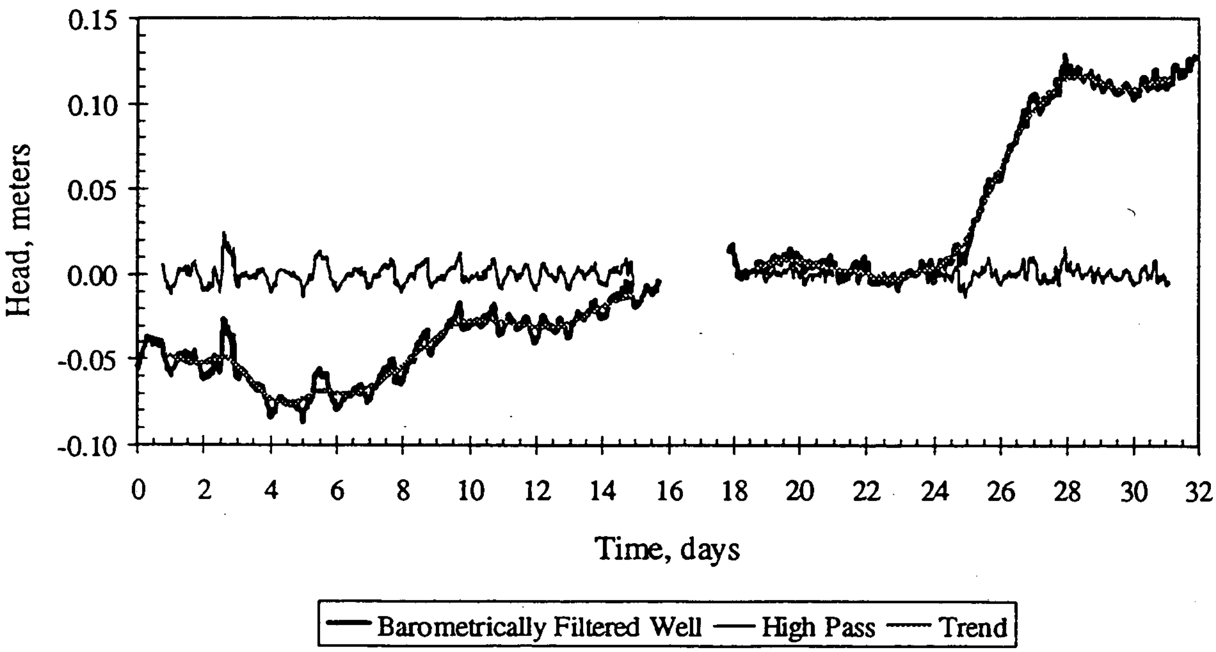


Figure 9: High-pass filter applied to barometrically filtered water levels of well EW-712.

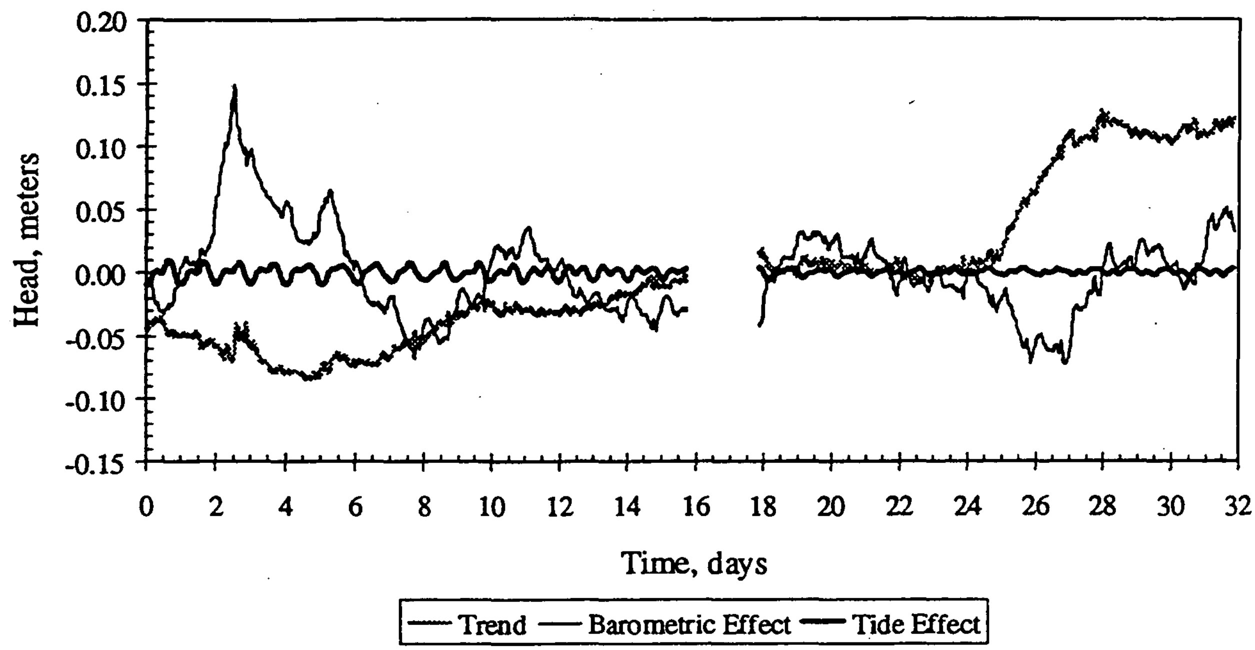


Figure 10: Least-squares filtering of water levels in well EW-712.

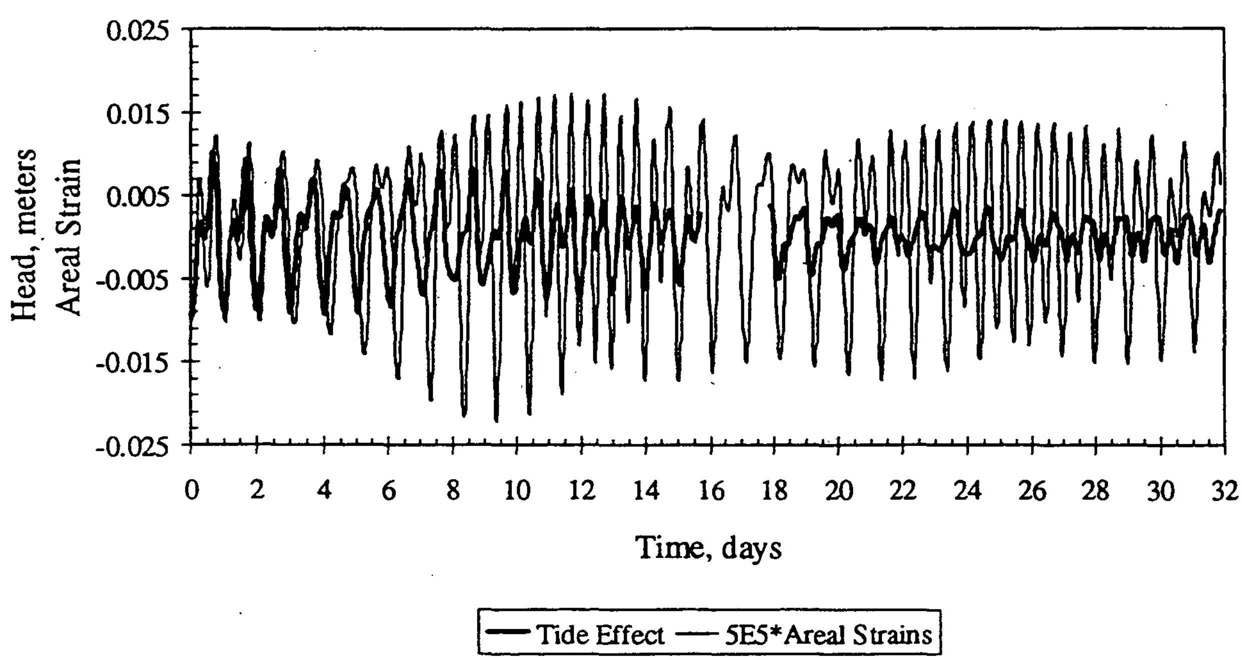


Figure 11: Areal strains and water level changes due to earth tide effects from least-squares filter for well EW-712.

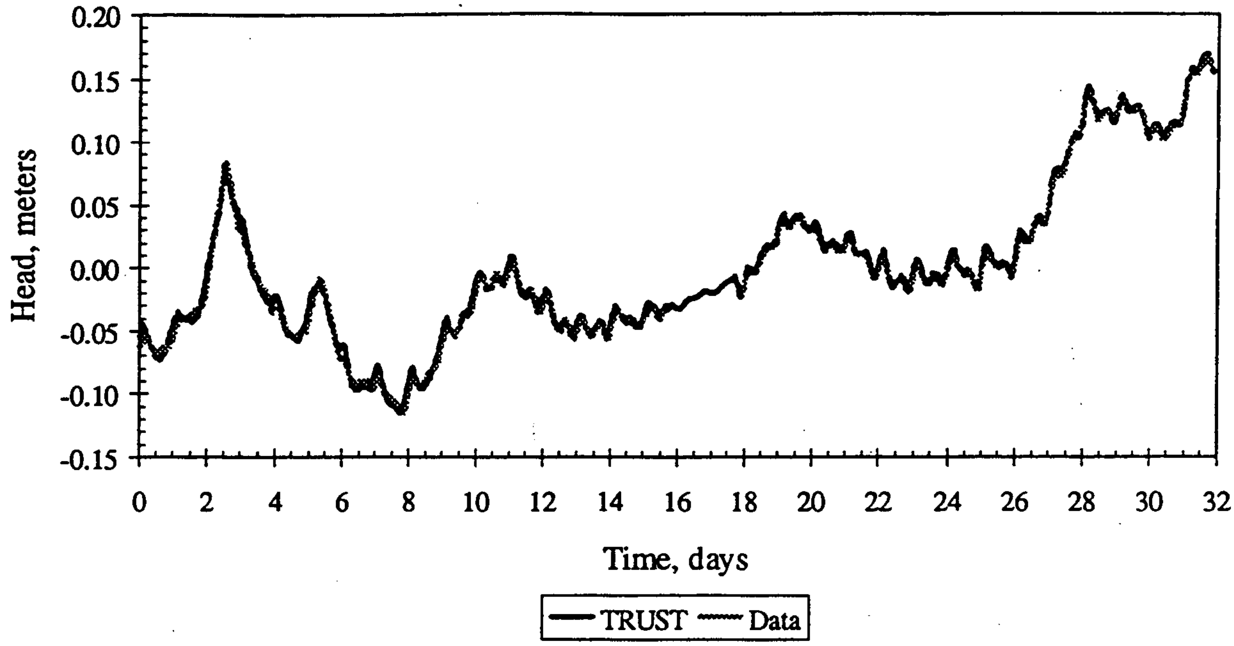


Figure 12: Best match with TRUST for barometric and earth tide analysis for well EW-712.

ERNEST ORLANDO LAWRENCE BERKELEY NATIONAL LABORATORY
ONE CYCLOTRON ROAD | BERKELEY, CALIFORNIA 94720

Prepared for the U.S. Department of Energy under Contract No. DE-AC03-76SF00098